Research Article

An acetylated Lysine Residue of Its Low-glucose Inhibitory Domain Controls Activity and Protein Interactions of ChREBP

Konstantin M. Petricek [1,2], Marieluise Kirchner [3], Manuela Sommerfeld [1], Heike Stephanowitz [4], Marie F. Kiefer [1], Yueming Meng [1], Sarah Dittrich [1], Henriette E. Dähnhardt [1], Knut Mai [2,5,6], Eberhard Krause [4], Philipp Mertins [3], Sylvia J. Wowro [1,†], and Michael Schupp [1,*,†]

*1 - **Institute of Pharmacology,** Max Rubner Center (MRC) for Cardiovascular Metabolic Renal Research, Charité-Universitätsmedizin Berlin, Corporate Member of Freie Universität Berlin, Humboldt-Universität zu Berlin, Berlin, Germany*

*2 - **Department of Endocrinology and Metabolism,** Charité-Universitätsmedizin Berlin, Corporate Member of Freie Universität Berlin, Humboldt-Universität Zu Berlin, and Berlin Institute of Health, European Reference Network on Rare Endocrine Diseases (ENDO-ERN), Berlin, Germany*

*3 - **Core Unit Proteomics,** Berlin Institute of Health at Charité – Universitätsmedizin Berlin and Max Delbrück Center for Molecular Medicine, Berlin, Germany*

*4 - **Leibniz-Forschungsinstitut für Molekulare Pharmakologie,** Berlin, Germany*

*5 - **German Center for Diabetes Research (DZD e.V.),** Neuherberg, Germany*

*6 - **Department of Human Nutrition,** German Institute of Human Nutrition Potsdam-Rehbrücke, Nuthetal, Germany*

***Correspondence to Michael Schupp:** Charité Universitätsmedizin Berlin, Institute of Pharmacology, 10115 Berlin, Germany. michael.schupp@charite.de (M. Schupp)*

https://doi.org/10.1016/j.jmb.2025.169189

Edited by Patrick Griffin

Abstract

Carbohydrate response element-binding protein (ChREBP) is a transcription factor activated by glucose metabolites that orchestrates the expression of genes involved in glycolysis, *de novo* lipogenesis, and ATP homeostasis. Inadequate ChREBP activity impairs the cellular adaptations to glucose exposure and in humans associates with dyslipidemia, fatty liver disease, and type 2 diabetes. ChREBP activity is regulated by cytosolic-nuclear translocation involving its low-glucose inhibitory domain (LID). Whether this domain is targeted by post-translational lysine acetylation is unknown. Here we report a novel LID acetylation site that controls activity and protein interactions of ChREBP. Mutation of this residue increased glucose-induced activity and target gene expression of ChREBP. Mechanistically, mutant ChREBP protein showed more nuclear localization and enhanced genomic binding to a target promoter. Interactions with proteins that exhibit differential binding upon glucose exposure were attenuated by the mutation, demonstrating the importance of the LID in the formation of the protein interactome. Particularly interactions with 14-3-3 proteins, factors that regulate cytosolic/nuclear trafficking of ChREBP, were reduced, whereas interactions with proteins of the nucleosome remodeling deacetylase complex (NuRD) were increased. These molecular insights may shape new therapeutic strategies to target ChREBP activity and counteract metabolic diseases.

Introduction

Carbohydrates represent one of the three major classes of macronutrients in our diet. Since a significant amount of carbohydrates is either ingested directly as simple sugars or absorbed as such, evolution has evolved mechanisms to appropriately sense and process glucose metabolites at the cellular level. One of these sensors is carbohydrate response element-binding protein (Mlxipl, MondoB, or Wbscr14, here referred to as ChREBP), a transcription factor activated by glucose metabolites that belongs to the Mondo family of basic helix-loop-helix transcription factors [1–3]. ChREBP is robustly expressed in liver, white and brown adipose tissue, muscle, kidney, pancreas, and the small intestine [4].

Activation of ChREBP adjusts glucose metabolite utilization to its availability by transcriptional regulation of genes involved in glycolysis and *de novo* lipogenesis [5] via binding to E-boxes in promoter and enhancer regions of these genes [6–8]. Moreover, ChREBP prevents toxicity of high glucose exposure by controlling genes that regulate cellular ATP homeostasis [9]. ChREBP deletion in mice leads to impaired glucose tolerance, insulin resistance, and an intolerance towards simple carbohydrates, resulting in hypothermia and death when fed on high-sucrose or fructose diets [4]. Insights from human studies that investigated expression, single nucleotide polymorphisms, or common variants of ChREBP support its pivotal role in glucose and fatty acid metabolism and related human pathologies [10–16]. Moreover, rare human missense variants of ChREBP were linked to higher incidences of type 2 diabetes [17].

The regulation of cellular ChREBP activity is via complex and yet incompletely understood interactions between binding proteins (e.g. 14-3-3 proteins, exportins, and importins), post-translational modifications (PTMs) (e.g. phosphorylation, O-GlcNAcylation, acetylation, and proline-hydroxylation) and metabolite exposure (e.g. glucose metabolites, ketone bodies, and AMP) which, in part interdependently, control cytosolic/nuclear translocation of ChREBP [18–23]. Moreover, additional mechanisms for its activation besides cytosolic to nuclear translocation are likely to exist since mutant forms of ChREBP with exclusive nuclear localization can retain glucose-responsiveness, and because forced nuclear accumulation not necessarily increases activity [24–26]. Future studies to characterize potential glucose-6 phosphate binding to ChREBP, which has been postulated to act as allosteric modulator [27], may help elucidating a more complete understanding of ChREBP activation.

Post-translational acetylation of ChREBP protein with functional relevance occurs on K672 in a p300 cofactor-dependent manner [28]. This acetyltransferase was shown earlier to physically interact with ChREBP [29]. Acetylation of K672, which is localized within its C-terminal DNA binding domain, was required for maximal DNA binding and activation of a luciferase reporter and ChREBP target gene expression in hepatocytes upon exposure to high glucose concentrations [28]. Increased K672 acetylation, at least in part, also mediates the activation of ChREBP by ethanol [30].

Whether acetylation targets lysine residues outside of the DNA binding domain of ChREBP is unknown. Interestingly, mutation of K672 to arginine reduced total ChREBP acetylation only partially [28], implying the presence of additional acetylation sites.

Here, we report two novel acetylation sites in the low-glucose inhibitory domain (LID) of ChREBP. This domain, together with the glucose-response activation conserved element (GRACE), is part of a conserved N-terminal glucose-sensing module (GSM) of Mondo proteins that confers glucose responsiveness via intra-and intermolecular interactions [24,26]. Mutation of one of these sites, K171, was functionally relevant and increased nuclear localization and genomic binding and, in turn, ChREBP reporter activity and target genes expression. In regard to the entire ChREBP protein interactome, which we show to consist of several hundred proteins in our experimental setup, the mutation reduced the number of interacting proteins with differential binding upon glucose exposure. Moreover, mutation of K171 decreased interactions with 14-3-3 proteins which regulate cytosolic/nuclear translocation and increased previously unknown interactions with components of the NuRD complex. Thus, our findings demonstrate the importance of K171 for ChREBP activity and the formation of the protein interactome. This may allow for identifying new strategies to target dysregulated ChREBP activity in metabolic diseases.

Materials and Methods

Materials

Chemicals, if not described otherwise, were purchased from Sigma-Aldrich/Merck. Cell culture reagents like antibiotics, trypsin, and fetal bovine serum (FBS) were purchased from Thermo Fisher Scientific. siRNA oligonucleotides were acquired from Eurogentec (Liège, Belgium), HEK293 cells (RRID: CVCL_0063) and AML12 hepatocytes (RRID:CVCL_0140) from ATCC (USA).

Cell culture and transient transfections

HEK293 cells and AML12 hepatocytes were cultured according to the manufacturer's instructions. Glucose concentrations in cell culture media for glucose sensing experiments were as indicated. AML12 cells lacking endogenous ChREBP were generated as detailed previously [25]. For Co-immunoprecipitation, subcellular frac-

tionation, and chromatin immunoprecipitation cells were transfected by $Ca_3(PO_4)_2$ precipitation. Per each transfection 6 μg plasmid, 450 μl CaCl 240 mM and 450 μl 2xBBS buffer (50mM N,N-Bis(2–hydroxyethyl)-2-aminoethanesulfonic acid, 280 mM NaCl, 1.5 mM Na_2HPO_4) were mixed thoroughly by vortexing and incubated at room temperature for 15 min. The transfection mixture was then added dropwise on cells cultured in 10 cm dishes. Determination of protein and mRNA expression as well as luciferase assay were performed on AML12 hepatocytes and HEK293 cells that were cultured in 24-well dishes and transiently transfected using Lipofectamine 2000 (Thermo Fisher Scientific) according to the manufacturer's instructions.

Site-directed mutagenesis of ChREBP

Expression plasmids for murine ChREBPα lysine mutants were generated by using the QuikChange II XL site-directed mutagenesis kit (Agilent) with the pCMV4-mChREBPα-FLAG vector and specific primers for amplification. Mutations were validated by Sanger sequencing. Primer sequences are listed in Suppl. Table S5.

Immunoblotting and densitometry

Whole cell proteins were isolated and homogenized in RIPA buffer by standard methods, sonicated, and separated by SDS PAGE before blotting to PVDF membranes by overnight tank blots. Protein concentrations were determined by the BCA assay (Thermo Fisher Scientific). After incubation with antibodies for ChREBP (#NB400-135, lot S2, Novus Biologicals), ACTB (#sc-47778, Santa Cruz), histone 3 (H3) (#06-755, Merck Millipore), pan-14-3-3 (#sc-1657 (H8), Santa Cruz), or GAPDH (#2118, Cell Signaling), a secondary horseradish peroxidase-conjugated antibody was added (Pierce) and a chemiluminescent substrate assay (Thermo Fisher Scientific) used for visualization. ImageJ was used for densitometry [31].

RNA isolation, cDNA synthesis and qPCR

RNA was purified by spin column kits (Macherey-Nagel, Germany). cDNA was synthesized with MMLV-RT (Promega). qPCRs were performed using SYBR Green qPCR MasterMix (Eurogentec) and evaluated according to the standard curve method for each transcript amplification. mRNA expression data were normalized to human *HPRT* expression and ChIP data were normalized to human *PPIB* abundance. Primer sequences are listed in Suppl. Table S5.

Luciferase reporter assays

Cells were transfected with wt or mutated pCMV4-mChREBPα-FLAG, pCMV4-Mlx, and a luciferase reporter that contained 2 copies of the *Acc1* ChoRE in its promoter driving firefly luciferase expression (pGL3-Acc1-ChoRE-luc) [32] by Lipofectamine 2000 overnight in media containing 25 mM of glucose. The next morning, cells were switched to media containing 2.5 mM glucose for 6 h before exposing cells to either 2.5 or 25 mM glucose for 24 h. Cells were harvested and luciferase activity determined. Luciferase reporter activity was normalized to co-expressed Renilla luciferase (Dual Luciferase, Promega).

Subcellular fractionation

Cells were washed, then scraped off in ice cold PBS and pelleted using centrifugation. Cell pellets were homogenized in hypotonic lysis buffer (10 mM HEPES, 0.34 M Sucrose, 10 mM KCl, 1.5 mM $MgCl_2$, 10% glycerol), vortexed every 5 min during a 45 min incubation on ice, and centrifuged at 7,500 g for 15 min at 4 °C (=cytosol). The pellet was washed twice with PBS and resuspended in RIPA buffer (=nuclear fraction).

FLAG-co-immunoprecipitation (IP)

After exposing to different glucose concentrations, transfected HEK293 cells were lysed in 1 ml IP lysis buffer (50 mM Tris-HCL, pH 7.5, 150 mM NaCl, 1 mM $MgCl_2$, 1% IGEPAL-CA-630, 0.5% sodium deoxycholate, 0.1% SDS and protease inhibitor tablet (Roche)) + 150U Benzonase by vortexing every 5 min during a 30 min incubation on ice. After 15 min centrifugation at 13,000 rpm in a benchtop centrifuge at 4 °C, supernatant was collected and protein concentration determined. Co-IP was performed with 450 μg of protein in a total volume of 1 ml (IP lysis buffer). FLAG-IP was performed with a 40 μl 50% slurry of anti-FLAG M2 Affinity gel (Sigma-Aldrich) for 2 h at 4 °C. Beads were collected by centrifugation and washed five times with 1 ml of wash buffer (50 mM Tris–HCL, pH 7.5, 150 mM NaCl, 1 mM $MgCl_2$ and protease inhibitor tablet (Roche)).

Chromatin immunoprecipitation (ChIP)

ChREBP ChIP in HEK293 cells with ectopic expression of wt or mutated ChREBP was performed as described elsewhere [33], using 2.5 μg ChREBP antibody (#NB400-135, lot S2, Novus Biologicals) per IP.

Detection of post-translational modifications by liquid chromatography-tandem mass spectrometry (LC-MS/MS)

Proteins were IP-enriched and subjected to LC-MS/MS analysis using an UltiMate 3000 RSLC nano LC system coupled on-line to an Orbitrap Elite mass spectrometer (Thermo Fisher Scientific) as previously described [25]. Mass spec-

tra were acquired in a data-dependent mode with one MS survey scan with a resolution of 60,000 (Orbitrap Elite) and MS/MS scans of the 15 most intense precursor ions in the linear trap quadrupole. Data were searched against the Uniprot mouse protein database (12/2014, 52,492 sequences; 24,959,523 residues). The mass tolerance of precursor and sequence ions was set to 20 ppm and 0.35 Da, respectively.

ChREBP interactome analyses by LC-MS/MS and data processing

After FLAG-IP, protein complex-containing beads were processed for analyses with LC-MS as follows: digestion buffer (6M urea/2 M thiourea in 50 mM ammonium bicarbonate) was added to the beads. Dithiothreitol (10 mM final concentration) was added and beads were incubated at RT for 30 min (reduction step). Chloroacetamide (55 mM final concentration) was added for 45 min (alkylation step). 500 ng endopeptidase LysC (Wako, Neuss) per sample was added and incubated for 4 h at RT. Samples were diluted with 50 mM ammonium bicarbonate (1:4) and 1 μg sequence grade trypsin (Promega, Mannheim, GER) was added (tryptic digest of proteins). Samples were digested overnight at RT. Samples were acidified with formic acid (final concentration 1%) and peptides were extracted and desalted using the StageTips protocol (C18 matrix). Peptides were separated by reversed phase chromatography on an in-house manufactured 20 cm fritless silica microcolumns with an inner diameter of 75 μm, packed with ReproSil-Pur C18-AQ 1.9 μm resin (Dr. Maisch GmbH) using a 98 min gradient with a 250 nl/min flow rate of increasing acetonitrile concentration on a High Performance Liquid Chromatography (HPLC) system (ThermoFischer Scientific). Eluting peptides were directly ionized by electrospray ionization and transferred into a Thermo QExactive Plus mass spectrometer. The instrument was operated in the data-dependent mode with performing full scans (70 K resolution; 3 × 106 ion count target; maximum injection time 50 ms), followed by top 10 MS2 scans using higher-energy collision dissociation (NCE of 26; 17.5 K resolution, 5 × 104 ion count target; 1.6 *m/z* isolation window; maximum injection time: 250 ms). Only precursors with charge states between 2 and 7 were fragmented. Dynamic exclusion was set to 30 sec.

Raw data were analyzed using the MaxQuant software (v1.6.3.4). The internal Andromeda search engine was used to search MS2 spectra against a human decoy UniProt database (HUMAN.2019-07) and FLAG-tagged murine wt and K171R ChREBP sequences, containing forward and reverse sequences. The search included variable modifications of oxidation (M) and N-terminal acetylation, deamidation (N and Q), and fixed modification of carbamidomethyl cysteine. Minimal peptide length was set to 7 amino acids and a maximum of two missed cleavages was allowed. The FDR was set to 1% for peptide and protein identifications. The integrated label-free quantification algorithm was activated. Unique and razor peptides were considered for quantification. Retention times were recalibrated based on the built-in nonlinear time-rescaling algorithm and MS/MS identifications were transferred between LC-MS/MS runs with the "Match between runs" option, in which the maximal retention time window was set to 0.7 min. The resulting text files were used for further analyses using the Perseus software package (v. 1.6.2.1). LFQ intensity values were used for quantification. Reverse hits, contaminants and proteins only identified by site were filtered out. Biological replicates for each condition were defined as groups and intensity values were filtered for "minimum value of 3" per group. After log2 transformation missing values were imputed with random noise simulating the detection limit of the MS. Differential protein abundance was calculated using two-sample Student's *t* test (cut off for interactor definition (against control): FDR 5%; cut off for differential interactors between conditions: FDR 10%).

Listings of physical ChREBP interactions were extracted from popular protein–protein interaction databases BioGRID [34], STRING [35] (medium confidence interaction score 0.400, max interactors in 1st shell 100), IntAct [36] and complemented with findings from a literature search. Databases were accessed September 10th, 2024. Venn diagrams were generated using BioVenn [37]. Following (differential) binder definition, an orienting enrichment analysis was performed on proteins that interacted with both wt and K171R ChREBP. For this a gene list was uploaded into the Enrichr webtool (maayanlab.cloud/Enrichr/) using default settings without an additional background [38]. Further interactome data analyzes were performed in R (version 4.3.2). In a first step UniProt gene symbols were derived from UniProt gene IDs using biomaRt (Bioconductor package, version 2.58.2). Depicted heatmaps were created using pheatmap (version 1.0.12), where "canberra" was used to compute row distance before clustering and "ward.D2" as clustering method. GO term analyses were performed using gprofiler2 (version 0.2.3) as stated (user_threshold = 0.05, correction_method = "fdr"). Next, identified terms were grouped by Resnik semantic similarity measurement using rrvgo (Bioconductor package, version 1.14.2) [39]. Finally, terms were sorted by adjusted p-value and ggplot2 library (version 3.5.0) was used for visualization of the results.

Statistical analyses

For cell culture experiments, representative results of at least 3 independent experiments performed in triplicates are shown and presented as mean ± sem. Significance was determined by

ANOVA and Sidak's correction for multiple testing and $P < 0.05$ was deemed significant ($^*P < 0.05$). Graphpad Prism Version 7/8 (Dotmatics) was used for statistical calculations.

Results

Ectopically expressed ChREBPα in HEK293 cells is acetylated at lysines 139 and 171 of the LID

Murine, FLAG-tagged ChREBPα was ectopically expressed in HEK293 cells and enriched by FLAG-immunoprecipitation (IP) (Figure 1A). Tryptic ChREBP fragments were analyzed by liquid chromatography-tandem mass spectrometry (LC-MS/MS). Sequence coverage was >70% (Figure 1B) and observed mass shifts and fragmentation profiles identified K171 and K139 as acetylated peptides (Figure 1C–E and Suppl. Figure S1A, B). Earlier reported acetylation of K672 and of two nearby lysines [28] were not detected in this experimental setup. This might be due to differences in the analyzed cell material (HEK293 versus HepG2) and cell culture conditions, the strength of ChREBP overexpression, and co-transfection of the acetyltransferase p300 in the earlier study [28]. Both newly identified residues localize to the LID and specific Mondo Conserved Regions (MCRs) of ChREBP [24,40,41], K139 to MCR III and K171 to MCR IV (Figure 1F). The shorter and transcriptionally more active ChREBPβ [42] does not contain either residue since this isoform is truncated at the N-terminus, lacking most of the LID (Figure 1F). Both identified lysine residues are highly conserved in mammals and birds and K171 falls within a bipartite nuclear localization signal (NLS) of MCR IV [43] (Figure 1G).

Mutation of K171 enhances ChREBP activity

Wild-type (wt) and lysine to arginine point mutations of ChREBP were expressed in HEK293 cells. We chose arginine because of similar chemical/steric characteristics compared to lysine without being acetylated. With comparable mRNA levels (Figure 2A), protein expression of mutated ChREBP was similar to wt expression (Figure 2B), suggesting that an amino acid exchange of the respective lysine residues to arginine does not affect protein stability. A co-transfected carbohydrate response element (ChoRE)-driven luciferase reporter showed increased transcriptional activity of K171R ChREBP, but not of the K139R mutant, at both low and high glucose concentrations (Figure 2C). Consistently, glucose-inducibility of *TXNIP* mRNA expression, known to be one of the most responsive ChREBP target genes [25,42,44], was increased (Figure 2D). Glucose inducibility of another target gene, *RGS16* [42,45], was also increased, albeit to a lesser extent (Suppl. Figure S2).

We next asked whether increased activity of ChREBP with K171R mutation could be replicated with an exchange of K171 to alanine. Indeed, ectopically expressed K171A ChREBP protein was readily detectable in HEK293 cells (Figure 2E) and, similar to K171R ChREBP, enhanced ChoRE reporter activity at high glucose concentrations (Figure 2F). This shows that the increased activity of mutated ChREBP is due to the loss of K171 rather than the insertion of a different amino acid. Notably, the same K171A mutation did not affect ChREBP activity in hepatocellular carcinoma HepG2 cells [23], perhaps due to differences in the experimental setup used.

We then tested the activity of K171R ChREBP in a more physiological context than HEK293 cells, which endogenously have no detectable ChREBP protein (Figure 2B). AML12 cells, a non-transformed mouse hepatocyte cell line transgenic for transforming growth factor alpha [46] and in which ChREBP was deleted by CRISPR/Cas9 [25], were transfected with vectors encoding wt and K171R ChREBP. With either protein expressed (Figure 2G), K171R ChREBP led to increased activity of the co-transfected ChoRE-driven luciferase reporter upon exposure to low or high glucose concentrations (Figure 2H). Together, these findings show that mutation of K171 increases ChoRE-driven luciferase reporter activity and target gene expression, indicating that the presence of K171 and/or its acetylation may associate with lower ChREBP activity.

Mutation of K171 increases nuclear localization and genomic binding of ChREBP

ChREBP transcriptional activity requires nuclear translocation and binding to DNA. We therefore investigated if the mutation affects the subcellular localization of ChREBP and its binding to a target promoter. Wt and K171R ChREBP were expressed in HEK293 cells and total ChREBP protein levels were comparable (Figure 3A and the densitometric analysis in Figure 3B of 3 independent experiments). Cytosolic ChREBP abundance tended to be lower in cells expressing the K171R mutant but did not reach significance (Figure 3A and the densitometric analysis in Figure 3C, left panel of 3 independent experiments). In contrast, mutation of K171 increased the abundance of ChREBP in the nuclear fraction at 2.5 and 25 mM of glucose (Figure 3A and its densitometric analysis in Figure 3C, left right panel).

Next, we analyzed binding of wt and K171R ChREBP to a known binding site in the proximal promoter of the *TXNIP* gene [7] by chromatin immunoprecipitation (ChIP). As expected, we found that ChREBP binding was glucose-dependent and that the mutation of K171 led to even higher enrichment of this genomic site in the ChREBP ChIP when cells were exposed to 25 mM of glucose (Fig-

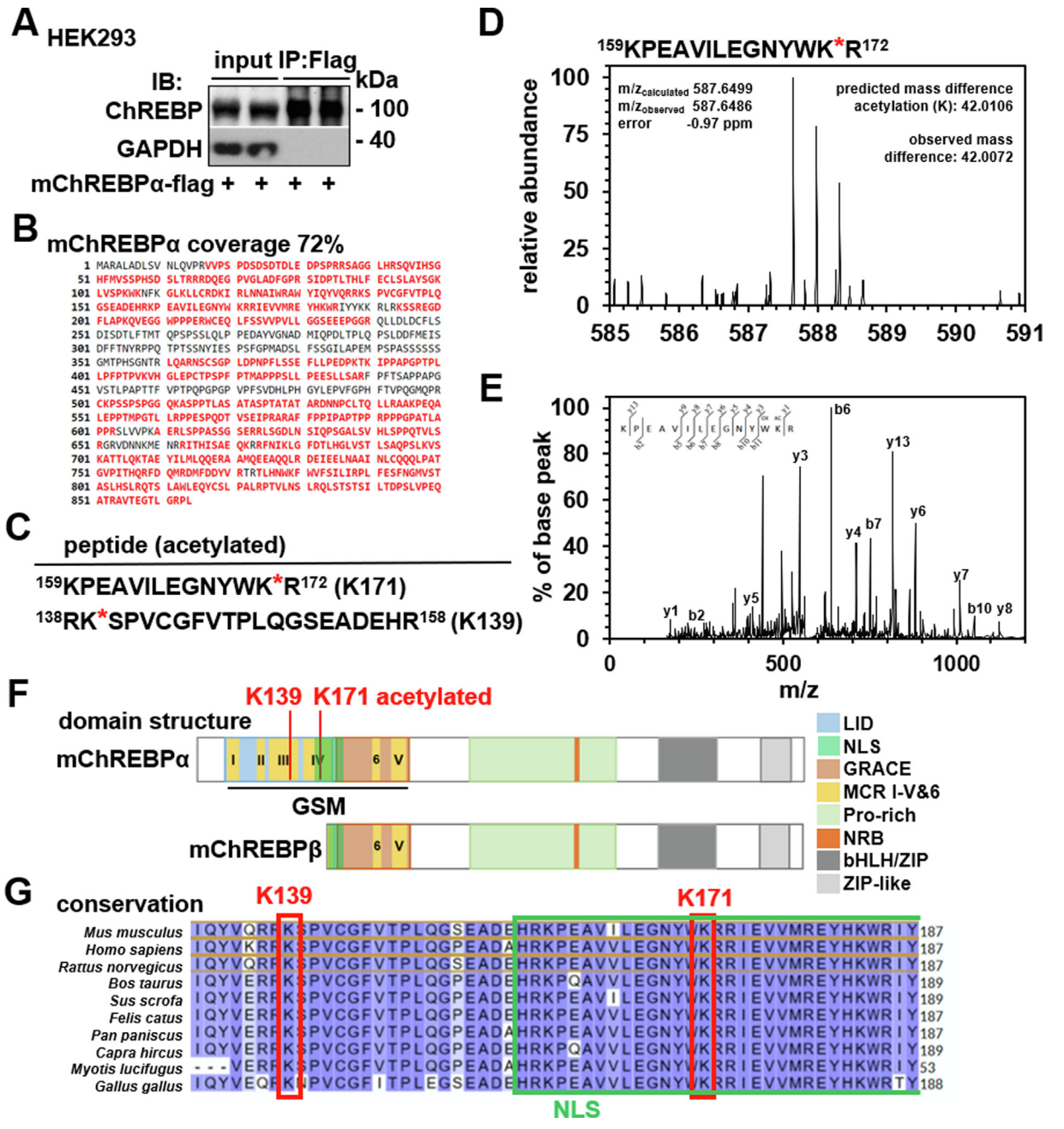

Figure 1. Ectopically expressed ChREBPα in HEK293 cells is acetylated at lysines 139 and 171. HEK293 cells were transfected with a vector encoding murine ChREBPα-flag. Input and Flag-IP analyzed for ChREBP protein by immunoblotting. GAPDH served as loading and IP control. (B) Sequence coverage of detected ChREBP peptides. (C) ChREBP peptides with acetylation of lysine residues. MS spectrum (D) and MS/MS fragment ion spectrum (E) of the peptide ^{159}KPEAVILEGNYWK*R^{172} of acetylated ChREBP. The peak with *m/z* 587.6486 in the MS spectrum corresponds to the triple charged ion of the lysine-acetylated sequence. Fragment ions resulting from the triple-charged precursor ion correspond to the ChREBP sequence. (F) Schematic depiction of ChREBPα and β domain structures with low-glucose inhibitory domain (LID), nuclear localization signal (NLS), glucose-response activation conserved element (GRACE) that form the glucose-sensing module (GSM), mondo-conserved regions (MCR) I-V&6, proline-rich region, LxxLL nuclear receptor box (NRB), basic helix-loop-helix-leucine zipper (bHLH/ZIP), and ZIP-like domains. (G) Conservation of acetylated lysine residues in mammals and birds.

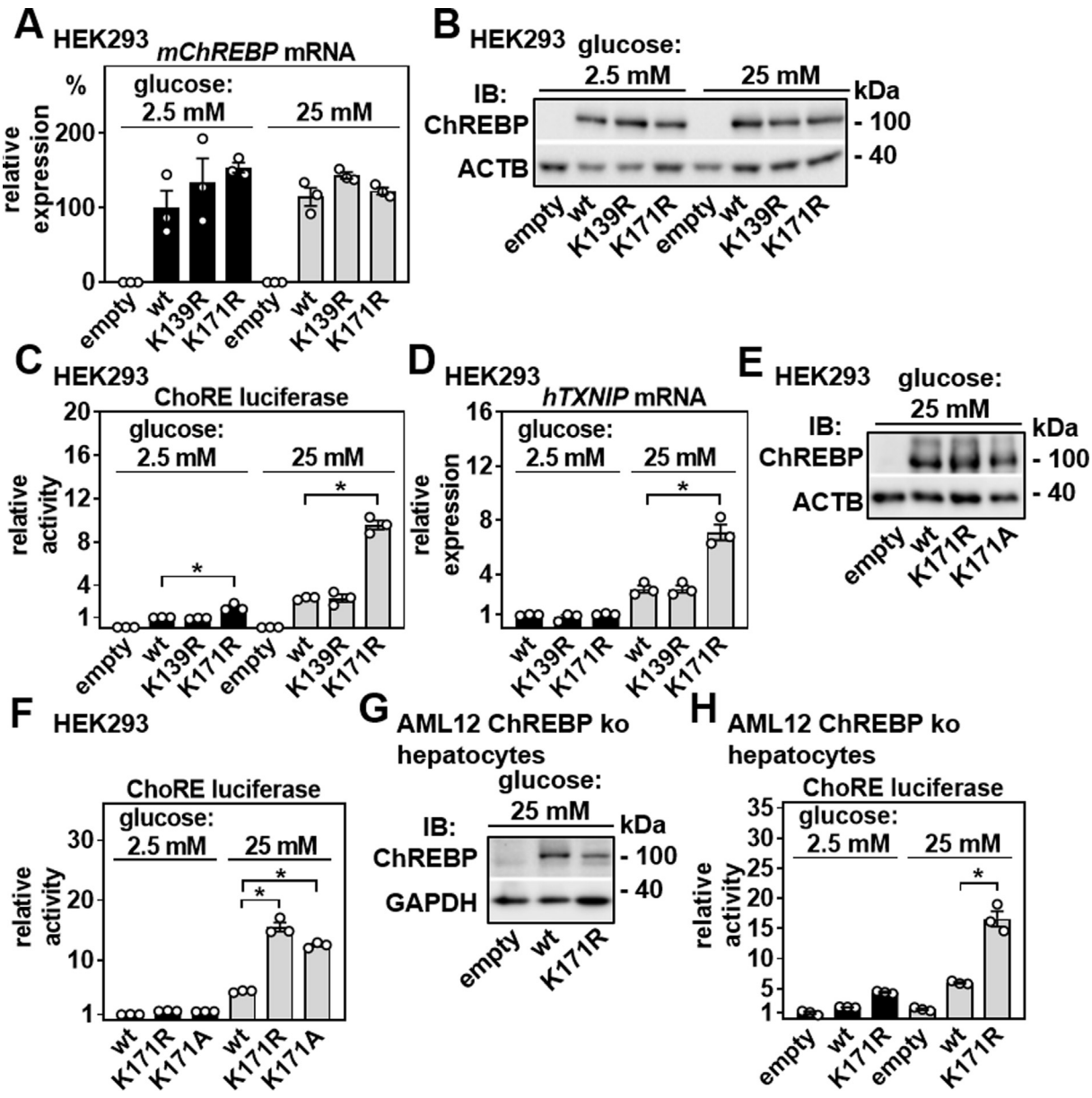

Figure 2. Mutation of K171 enhances ChREBP activity. (A) HEK293 cells were transfected with vectors encoding wt or mutated ChREBP and exposed to 2.5 mM or 25 mM of glucose for 24 h and mRNA expression determined by qPCR. (B) ChREBP protein expression of cells described in (A) was analyzed by immunoblottiong. ACTB served as loading control. (C) Cells described in (A) were cotransfected with a ChoRE-driven luciferase reporter and analyzed for its activity. (D) Cells described in (A) were analyzed for mRNA expression of *hTXNIP* by qPCR. (E) HEK293 cells were transfected with vectors encoding wt or mutated ChREBP and its protein expression analyzed by immunoblottiong. ACTB served as loading control. (F) Cells described in (E) were cotransfected with a carbohydrate response element (ChoRE)-driven luciferase reporter, exposed to 2.5 mM or 25 mM of glucose for 24 h, and luciferase activity determined. (G) AML12 hepatocytes lacking ChREBP were transfected with with vectors encoding wt or mutated ChREBP and its protein expression analyzed by immunoblottiong. GAPDH served as loading control. (H) AML12 cells were cotransfected with a ChoRE-driven luciferase reporter, exposed to 2.5 mM or 25 mM of glucose for 24 h, and luciferase activity determined. Data are represented as individual data points and mean ± SEM and $^*P < 0.05$ vs. wt ChREBP-expressing cells by one-way ANOVA and Sidak's correction for multiple testing.

ure 3D). We conclude that the increased activity of K171R ChREBP is likely due to increased nuclear partitioning and genomic binding of the mutant protein.

Identifying the ChREBP protein interactome and its differential binding in HEK293 cells

We then investigated whether K171R mutation affects the protein interactome of ChREBP in

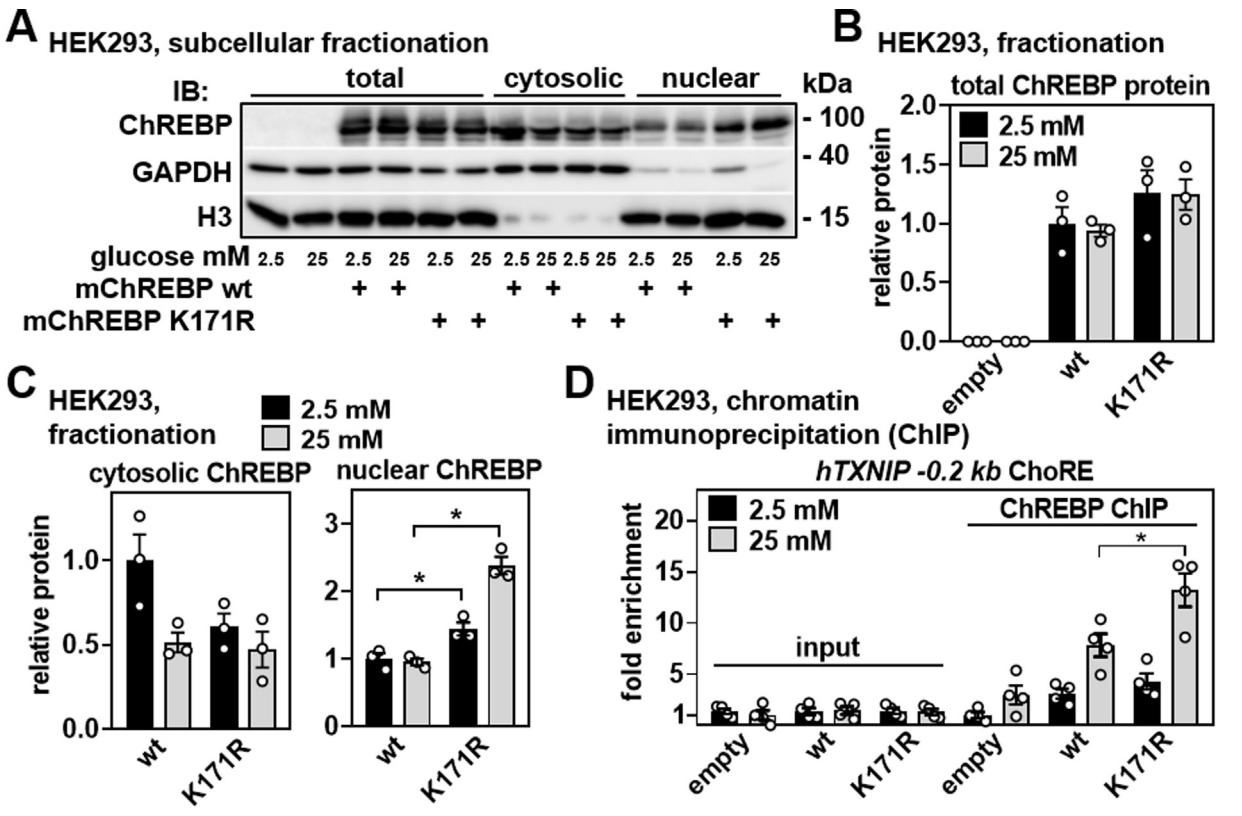

Figure 3. Mutation of K171 increases nuclear localization and genomic binding of ChREBP. (A) HEK293 cells were transfected with vectors encoding wt or mutated ChREBP and exposed to 2.5 mM or 25 mM of glucose for 24 h. Subsequently, subcellular fractions were isolated and cytosolic and nuclear proteins analyzed for ChREBP abundance by immunoblottinging. GAPDH and Histone H3 served as loading and fractionation controls. (B) Densitometric analysis of total ChREBP protein levels in cells described in (A) of 3 independent experiments. (C) Densitometric analysis of cytosolic and nuclear ChREBP protein abundance in cells described in (A) of 3 independent experiments. (D) Cells described in (A) were analyzed for ChREBP binding to a carbohydrate response element (ChoRE) upstream of the transcriptional start site of the *hTXNIP* gene by chromatin immunoprecipitation (ChIP). Data are represented as individual data points and mean ± SEM and $^*P < 0.05$ vs. wt ChREBP-expressing cells by one-way ANOVA and Sidak's correction for multiple testing.

HEK293 cells by LC-MS/MS. With an FDR of 5% we identified 410 proteins that interact with wt ChREBP and 437 proteins that interact with K171R ChREBP in our heterologous system, with an overlap of 333 proteins interacting with both (Figure 4A and Suppl. Table S1). Identified proteins include direct binders to ChREBP, such as 14-3-3 proteins, but likely also indirect binders that form bigger functional complexes without direct physical contact to ChREBP.

Next, we compared these proteins to previously reported ChREBP interactors. Of 54 proteins that were shown to interact with ChREBP previously (see method section for identification), 13 were detected (FDR 5%) in our dataset and most of them (10 proteins) showed binding to both wt and K171R ChREBP (Figure 4A and Suppl. Table S2). Enrichment analysis of the 333 proteins that interact with both wt and K171R ChREBP by Enrichr [38] yielded *cytosolic/nuclear trafficking, RAN cycling*, and *sumoylation* as top metabolic BioCarta pathways [47] (Figure 4B,top panel), which may be interconnected [48]. This underlines the relevance of interacting proteins for the control of ChREBP's subcellular localization and activity. Regarding peptide motifs, the *14-3-3 domain* was the most enriched InterPro sequence [49] among common interactors (Figure 4B, middle panel), presumably because of the detection of all seven 14-3-3 isoforms [50] (Suppl. Table S1). Examining underlying transcriptional regulatory relationships, we found that the anabolic transcription factor MYC was central to the expression of these proteins (Figure 4B, TRRUST [51] enrichment in the bottom panel). This suggests a tight integration of ChREBP and MYC functions, which not only belong to the same superfamily of Myc/Max/Mad factors but were also shown to depend on each other for adequate cellular glucose sensing, cell growth and proliferation, and aging [52–54].

We then analyzed proteins that interact differentially with wt or K171R ChREBP at 2.5 or

25 mM of glucose (FDR 10%). Intriguingly, heatmap clustering showed more pronounced glucose dependency of proteins interacting with wt ChREBP (n = 40) than those interacting with K171-mutated ChREBP (n = 43) (Figure 4C and Suppl. Table S3). Especially at low glucose conditions the interactome showed major differences between WT and K171R ChREBP (Figure 4C middle panel, Suppl. Table S3). In contrast, interactors of K171-mutated ChREBP showed a more constitutive interaction, irrespective of glucose concentrations (Figure 4C top panel). We performed prioritized TOP10 gene ontology (GO) term analyses using the Bioconductor package rrvgo [39,55] for ChREBP wt vs. K171R differential interactors at 2.5 mM of glucose, due to more pronounced differences at this condition. Regarding cellular components (CC), *nucleus-related terms* were enriched among interactors of both wt and K171R ChREBP (Figure 4D). In contrast, the terms *cytosol*, *cytoplasm*, and terms associated with *cytoskeleton dependent intracellular transport* were enriched only among interactors of wt ChREBP (Figure 4D). GO term analysis also revealed enrichment of the biological processes (BP) *microtubule cytoskeleton organization* and *cell cycle* for wt ChREBP and *RNA-related pathways* and *gene expression* for K171-mutated ChREBP (Suppl. Figure S3). GO terms of molecular function (MF) were more diverse among interactors of wt ChREBP and restricted to *RNA binding*, *organic cyclic compound binding* and *nucleic acid binding* among interactors of K171-mutated ChREBP, with *nucleic acid binding* enriched only for K171R ChREBP interactors (Suppl. Figure S3).

In addition, we identified a total of 26 proteins that exhibit significant differential interactions between 2.5 and 25 mM of glucose, with 17 proteins showing glucose-differential interactions for wt ChREBP and only 9 proteins for K171R ChREBP (FDR 10%, Suppl. Table S4). Heatmap clustering demonstrated that the ChREBP wt interactome shows a stronger response to glucose with differences primarily at 2.5 mM of glucose compared to the K171R ChREBP interactome (Figure 4E). Both GO:CC (Figure 4F) and BP terms (Suppl. Figure S4) were more diverse for glucose differential interactors of wt ChREBP, rooting partly in the larger number of wt interactors at this condition, and included many terms related to *cytoskeleton*, which were not enriched among interactors of K171R ChREBP.

Taken together, we identified a high number of novel proteins that interact with ectopically expressed ChREBP in HEK293 cells. Mutation of ChREBP K171 prevents interactions with proteins involved in cytosolic retention at low glucose concentrations and, on the other hand, drives glucose-independent/constitutive interactions with proteins involved in transcriptional events. In conclusion, these alterations in the protein interactome are highly indicative for increased activity of K171-mutated ChREBP.

Mutation of ChREBP K171 reduces physical interaction with 14-3-3 proteins and affects interaction with proteins involved in nuclear import and the NuRD complex

ChREBP contains several distinct binding sites for 14-3-3 proteins and physical interaction induces cytosolic retention or nuclear export of ChREBP [20,56,57]. As stated, we found that all seven known 14-3-3 isoforms interact with wt and K171R ChREBP (Suppl. Table S1 and Figure 5A). Binding to wt ChREBP tended to be glucose-dependent and stronger at 2.5 mM of glucose but did not reach statistical significance. However, overall binding to K171R ChREBP was significantly reduced for the 14-3-3 isoforms γ, η, and θ (YWHAG, YWHAH, and YWHAQ) when not differentiating between low and high glucose concentrations (FDR 10%, Figure 5A), implying that reduced binding to these 3 isoforms may account for increased activity of K171R-mutated ChREBP. Reduced binding of K171R-mutated ChREBP with 14-3-3 proteins were also observed when visualized by a pan-14-3-3 antibody that reacts with all isoforms (Figure 5B and its densitometric analysis in Figure 5C of 4 independent experiments).

Besides 14-3-3 proteins, we found that several importins, exportins and their respective subunits interact with wt and/or K171R ChREBP (Suppl. Table S1). Many of these proteins cluster to GO:BP terms related to protein import or export from the nucleus (Figure 5D, 5E). Notably, these GO:BP terms also include the GTP-binding nuclear protein RAN, involved in nucleocytoplasmic transport [58], which we found to interact with both wt and K171R ChREBP (Figure 5D, 5E). While there were no significant differences of enriched interactors involved in protein export from nucleus (Figure 5D), GO term-based examination showed that interactions of FLNA, MAVS, and IPO5 with K171R ChREBP were decreased with statistical significance when not differentiating between low and high glucose concentrations (FDR 10%, Figure 5E). GO term analysis of ChREBP interactors (Suppl. Table S1) also yielded nucleosome remodeling and deacetylase (NuRD) complex as enriched term, with MTA2 and HDAC2 interactions significantly stronger to K171R than wt ChREBP when not differentiating between low and high glucose concentrations (FDR 10%, Figure 5F). To our knowledge, this is the first time that proteins of the NuRD complex are identified as ChREBP interactors. We conclude that mutation of ChREBP K171 induces quantitative differences in the interaction with proteins that control its cytosolic/nuclear trafficking and transcriptional activity.

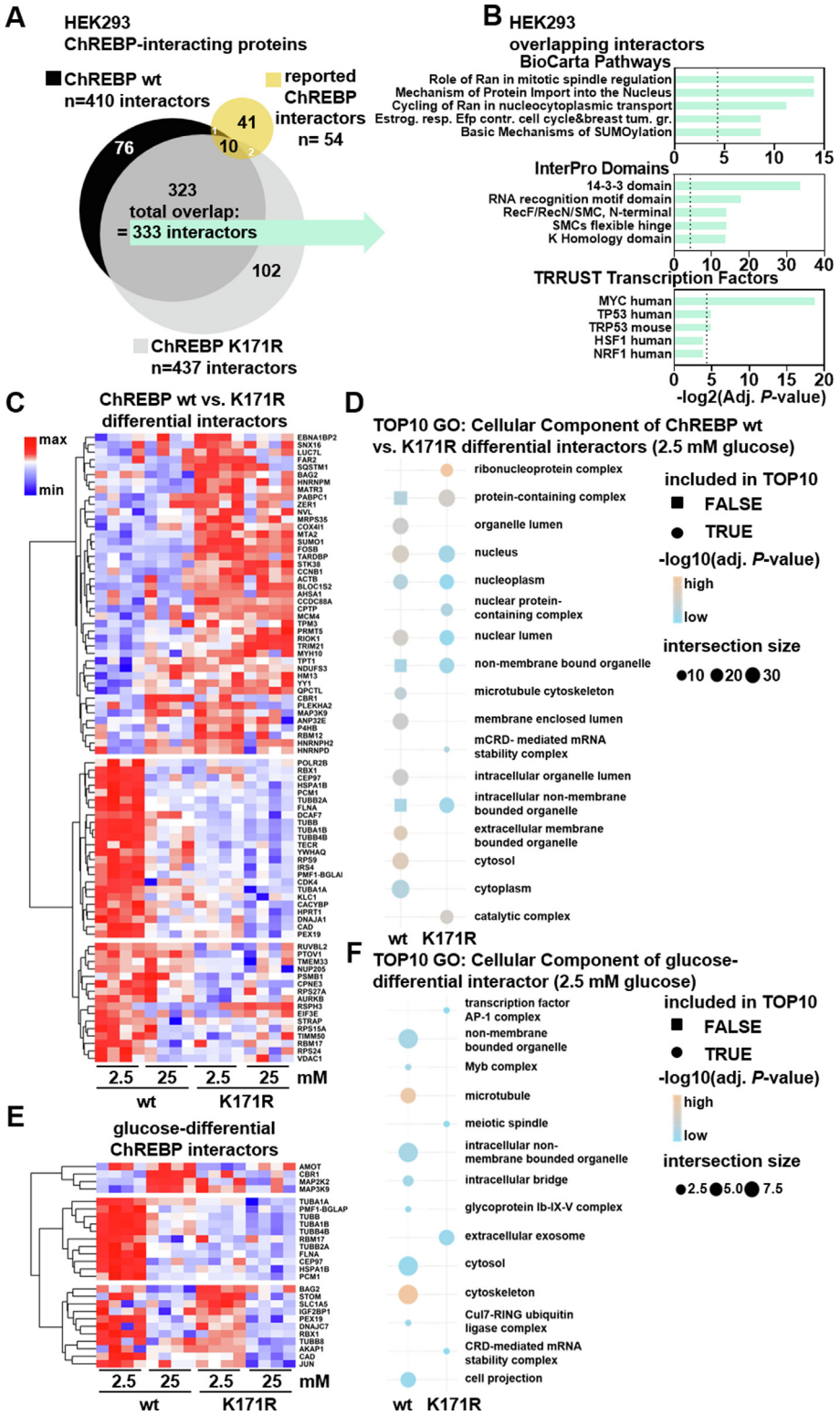
A
HEK293
ChREBP-interacting proteins
ChREBP wt
n=410 interactors
reported
ChREBP
interactors
n= 54
41
10
76
323
total overlap:
= 333 interactors
102
ChREBP K171R
n=437 interactors
B
HEK293
overlapping interactors
BioCarta Pathways
Role of Ran in mitotic spindle regulation
Mechanism of Protein Import into the Nucleus
Cycling of Ran in nucleocytoplasmic transport
Estrog. resp. Efp contr. cell cycle&breast tum. gr.
Basic Mechanisms of SUMOylation
0 5 10 15
InterPro Domains
14-3-3 domain
RNA recognition motif domain
RecF/RecN/SMC, N-terminal
SMCs flexible hinge
K Homology domain
0 10 20 30 40
TRRUST Transcription Factors
MYC human
TP53 human
TRP53 mouse
HSF1 human
NRF1 human
0 5 10 15 20
-log2(Adj. P-value)
C
ChREBP wt vs. K171R
differential interactors
max
min
2.5 25 2.5 25 mM
wt K171R
D
TOP10 GO: Cellular Component of ChREBP wt
vs. K171R differential interactors (2.5 mM glucose)
ribonucleoprotein complex
protein-containing complex
organelle lumen
nucleus
nucleoplasm
nuclear protein-
containing complex
nuclear lumen
non-membrane bound organelle
microtubule cytoskeleton
membrane enclosed lumen
mCRD- mediated mRNA
stability complex
intracellular organelle lumen
intracellular non-membrane
bounded organelle
extracellular membrane
bounded organelle
cytosol
cytoplasm
catalytic complex
wt K171R
included in TOP10
FALSE
TRUE
-log10(adj. P-value)
high
low
intersection size
10 20 30
E
glucose-differential
ChREBP interactors
2.5 25 2.5 25 mM
wt K171R
F
TOP10 GO: Cellular Component of glucose-
differential interactor (2.5 mM glucose)
transcription factor
AP-1 complex
non-membrane
bounded organelle
Myb complex
microtubule
meiotic spindle
intracellular non-
membrane bounded organelle
intracellular bridge
glycoprotein Ib-IX-V complex
extracellular exosome
cytosol
cytoskeleton
Cul7-RING ubiquitin
ligase complex
CRD-mediated mRNA
stability complex
cell projection
wt K171R
included in TOP10
FALSE
TRUE
-log10(adj. P-value)
high
low
intersection size
2.5 5.0 7.5

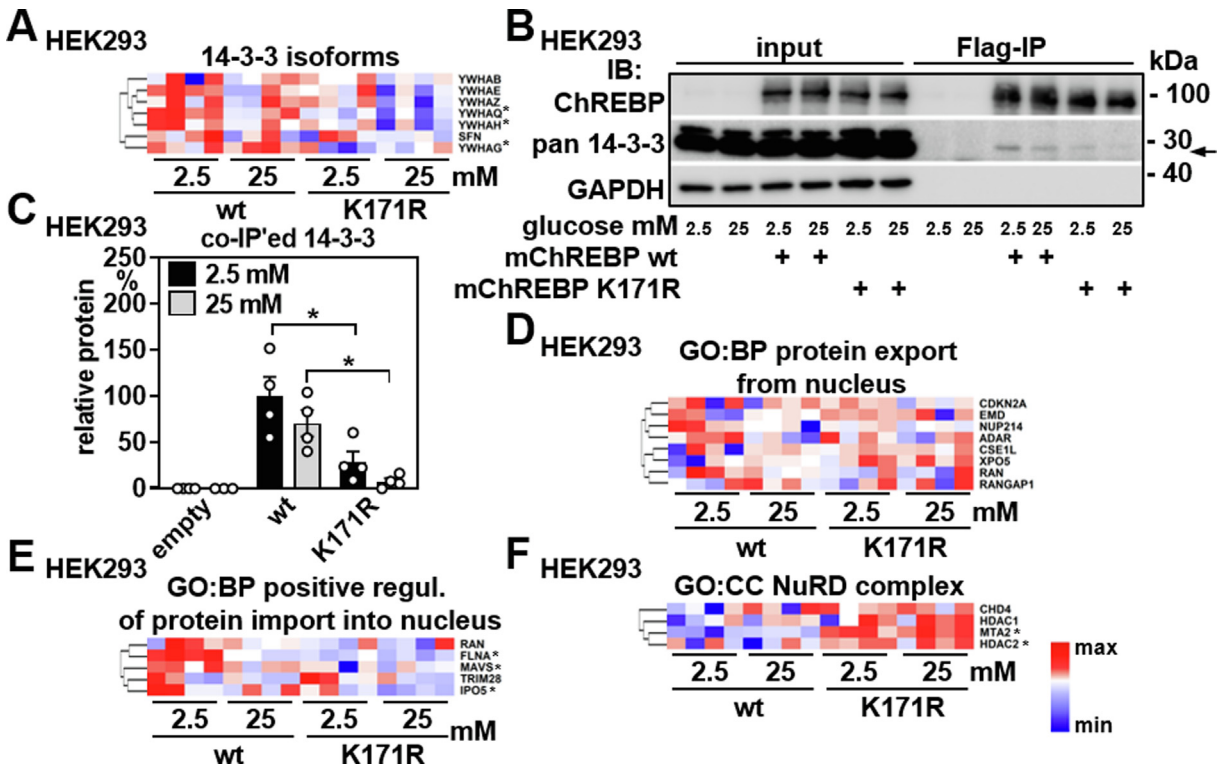

Figure 5. Mutation of ChREBP K171 reduces physical interaction with 14-3-3 proteins and affects interaction with proteins involved in nuclear import and the NuRD complex. HEK293 cells were transfected with vectors encoding Flag-tagged wt or mutated ChREBP and exposed to 2.5 mM or 25 mM of glucose for 24 h. (A) Flag-IP'ed proteins were analyzed by mass spectrometry (MassSpec) for interaction with 14-3-3 isoforms. (B) Flag-immunoprecipiated (IP) proteins were analyzed for ChREBP and 14-3-3 protein by immunoblotting. Flag-IP protein of empty vector-transfected cells served as negative control. GAPDH served as loading and IP control. (C) Densitometric analysis of co-IP'ed 14-3-3 protein shown in (B) of 4 independent experiments. (D-F) Clustered heatmaps of ChREBP-interacting proteins based on GO terms that relate to nuclear translocation (D, E) and the NuRD complex (F). In (C), data are presented as individual data points and mean ± SEM and with $*P < 0.05$ vs. wt ChREBP-expressing cells by one-way ANOVA and Sidak's correction for multiple testing. Differential protein abundance was calculated using student's *t* test with a cut off for interactor definition against control of FDR 5% and of FDR 10% for differential interactors between wt and K171R within the GO term.

Discussion

We discovered post-translational acetylation of a conserved lysine residue within the LID of ChREBP. Mutation of this K171 residue to arginine or alanine increased activity of a ChoRE-driven luciferase reporter and induced expression of ChREBP target genes. Enhanced activity was

Figure 4. Identifying the ChREBP protein interactome and its differential binding in HEK293 cells. HEK293 cells were transfected with vectors encoding Flag-tagged wt or mutated ChREBP and exposed to 2.5 mM or 25 mM of glucose for 24 h. Flag-immunoprecipitated (IP) proteins were analyzed by mass spectrometry. Flag-IP protein of empty vector-transfected cells served as negative control. (A) Venn diagram of total number of identified interacting proteins (FDR 5%). (B) Analysis of the Top 5-enriched pathways (top panel), protein domains (middle panel), and regulating transcription factors (bottom panel) of $n = 333$ proteins that interact with both wt and K171R ChREBP. Clustered heatmaps of (C) $n = 83$ proteins that show significant differential binding (FDR 10%) between wt and K171 ChREBP and (E) of $n = 26$ proteins that show significant differential binding between 2.5 mM and 25 mM glucose (FDR 10%) of wt ($n = 17$) or K171R ChREBP ($n = 9$). Top 10-simplified GO: Cellular Component terms of (D) ChREBP wt vs. K171R interactors and of (F) glucose differential interactors at 2.5 mM glucose. Differential protein abundance was calculated using student's *t* test with a cut off for interactor definition against control of FDR 5% and of FDR 10% for differential interactors between conditions. (D) and (F) depict FDR 5% TOP10 GO terms.

likely a result of more nuclear localization and increased genomic binding. Accordingly, K171-mutated ChREBP showed reduced interactions with 14-3-3 proteins that are known to confer cytosolic retention or nuclear export of ChREBP. Globally, mutation of K171 induced interactions with proteins related to gene expression at the expense of interactions with proteins involved in cytosolic retention at low glucose concentrations.

In sum, these data imply that the presence of K171 *per se* and/or K171 acetylation associate with reduced ChREBP activity, lower target gene expression, and increased binding to 14-3-3 proteins that induce cytoplasmatic retention. This is surprising since acetylation of the other residue, K672, increased ChREBP activity by enhancing DNA binding [28]. Residue-specific enzymatic activities for the acetylation of K171 and K672 that act in an environment-dependent manner may reconcile this discrepancy. In this context, acetylation of K672 was increased by the histone acetyltransferase p300 [28], which localizes predominantly to the nucleus. Which acetyltransferase(s)/deacetylase(s) control K171 acetylation and whether the modification occurs in the cytosol or the nucleus is currently unknown. One could speculate that the identified proteins of the NuRD complex, especially HDAC1/2 and the scaffolding protein MTA2, may interact with ChREBP for regulating its acetylation at K171. Nevertheless, although non-histone substrates for HDAC1 and HDAC2 exist [59–61], transcriptional regulation occurs primarily via deacetylating histones H3 and H4 [62]. Interestingly, K171 is part of the N-terminal LID and not the DNA binding domain, suggesting that lysine acetylation may reduce (K171) or enhance (K672) ChREBP activity, depending on the protein domain in which the modification occurs. At this point, however, it is hard to discern whether increased activity of K171-mutated ChREBP is due to the loss of this lysine residue and/or because of losing K171 acetylation and both scenarios appear plausible. Nevertheless, our data provides evidence for the physiological relevance of this residue for activity and protein interactions of ChREBP.

Intriguingly, K171 localizes to the bipartite NLS of the MCR IV. This region binds importin α, which is required for entering the nucleus upon exposure to high glucose concentrations [43]. Moreover, also 14-3-3 can bind to the NLS via the alpha3 helix (amino acids 169–190), competing with importin α binding and proposed to thereby regulate the subcellular localization of ChREBP [23,43]. The crystal structure of the ChREBP NLS peptide bound to importin α revealed polar interactions between the cluster of basic residues around K171 and tandem armadillo (ARM) 2–5 domains of importin α [23]. Specifically, K171 interacted via hydrogen bonds with T155 of importin α [23]. Based on this, acetylation of K171 may interfere with importin α binding and shift competitive binding of importin α and 14-3-3 towards the latter, resulting in lower ChREBP activity. Mutating K171 to arginine or alanine may induce the opposite effect. Indeed, K171-mutated ChREBP showed reduced interaction with some, but not all 14-3-3 isoforms. Moreover, interactions with different importin subunits were detected (Suppl. Table S1, KPNA2, KPNA3, KPNB1, IPO5, IPO7, and IPO8) but did not show a consistent pattern of regulation, which could be due to methodological limitations or the dynamics of these interactions in cells. Nevertheless, acetylation of K171 adds another layer to the complex and yet incompletely understood regulation of ChREBP activity.

Besides the directed analysis of 14-3-3 binding to ChREBP, we performed a global and unbiased interactome analysis and identified an unprecedented high number of new interacting proteins. Strikingly, we detected ∼25% (13 of 54) of all previously reported protein interactors of ChREBP, suggesting that our approach identified biologically relevant interactions, although with limitation that we will discuss in the next paragraph. Most interactors showed binding to both wt and K171-mutated ChREBP. Nevertheless, mutation of K171 diminished the binding of proteins involved in cytoplasmic retention at low glucose concentrations. This finding is consistent with more nuclear localization and higher activity of K171R ChREBP. It is tempting to speculate on cause versus consequence of these observations. We would favor a model where mutation of K171 interferes with 14-3-3 binding as a primary event that triggers more nuclear localization even at 2.5 mM of glucose. Consequentially, composition of the resulting ChREBP protein complex likely further adapts to its subcellular localization. Independent of these interactome characteristics for wt and K171-mutated ChREBP, this dataset provides a highly valuable repository of protein interactions to further dissect ChREBP biology.

A limitation of our study is the heterologous system we used for most experiments, consisting of human HEK293 cells with ectopic expression of FLAG-tagged murine ChREBP. In terms of interacting proteins, this may identify proteins that bind ChREBP primarily because of the robust ectopic expression, contributing at least in part to the high number of novel interactors. However, very similar heterologous systems were used in the past and findings usually translate well to the function of endogenous ChREBP in for instance hepatocytes or adipocytes [18,19,63,64]. Consistently, the increased activity of K171R ChREBP was not restricted to HEK293 cells and also detectable in a more physiological cellular context of AML12 hepatocytes. Further, heterologous systems can be controlled much more stringently, allowing fine-tuned expression of tagged proteins and tag-specific IP's, thus avoiding poor outcomes

due to ChREBP antibody limitations [25,63]. Also, the detection of lysine acetylation of ChREBP, perhaps in contrast to other, more abundant PTMs, is facilitated by using this heterologous system. Another limitation is in regard to the dynamics of K171 acetylation, which we could not assess due to the lack of a specific antibody for acetylated K171 of ChREBP and poor, unreproducible results using a pan-acetylated-lysine antibody (Cell Signaling #9681, lot. 14). Moreover, evidence for K171 acetylation of endogenously expressed ChREBP is also lacking, which remains to be dissected in future studies. Mass spectra of IP-enriched ChREBP from mouse liver did not indicate lysine acetylation [25], perhaps due to low abundance of the modified residue(s), low acetyltransferase/high deacetylase activities of liver tissue, or other methodological limitations. On the other hand, acetylation of ChREBP K171 was detected in the human cancer cell line NCI-H2228 [65] and is depicted at the PTM database PhosphoSitePlus (https://www.phosphosite.org/) [66], suggesting that this modification indeed targets the endogenously expressed protein.

Taken together, we identified an acetylated lysine residue within the LID of ChREBP that regulates activity and protein interactions of this pivotal glucose sensor. These molecular insights may help to develop new therapeutic strategies to target dysregulated ChREBP activity and metabolic diseases.

CRediT authorship contribution statement

Konstantin M. Petricek: Writing – review & editing, Writing – original draft, Visualization, Validation, Investigation, Funding acquisition, Formal analysis, Data curation, Conceptualization. **Marieluise Kirchner:** Visualization, Validation, Methodology, Investigation, Formal analysis, Data curation, Conceptualization. **Manuela Sommerfeld:** Investigation, Formal analysis, Data curation. **Heike Stephanowitz:** Methodology, Investigation, Data curation, Conceptualization. **Marie F. Kiefer:** Formal analysis, Data curation. **Yueming Meng:** Formal analysis, Data curation. **Sarah Dittrich:** Formal analysis, Data curation. **Henriette E. Dähnhardt:** Formal analysis, Data curation. **Knut Mai:** Supervision, Investigation, Conceptualization. **Eberhard Krause:** Methodology, Formal analysis, Conceptualization. **Philipp Mertins:** Methodology, Conceptualization. **Sylvia J. Wowro:** Writing – review & editing, Writing – original draft, Visualization, Supervision, Project administration, Methodology, Funding acquisition, Formal analysis, Data curation, Conceptualization. **Michael Schupp:** Writing – review & editing, Writing – original draft, Visualization, Supervision, Project administration, Investigation, Funding acquisition, Formal analysis, Conceptualization.

Funding

This work was supported by the German Research Foundation (DFG, grant nr. 415542650 to M.S. and grant nr. 502067018 to S.J.W. K.M.P was supported by the German Diabetes Society and the Sonnenfeld Foundation Berlin.

DATA AVAILABILITY

Data will be made available on request.

DECLARATION OF COMPETING INTEREST

The authors declare that they have no known competing financial interests or personal relationships that could have appeared to influence the work reported in this paper.

Acknowledgments

We thank Howard C. Towle (University of Minnesota, Minneapolis), for providing murine ChREBP expression vectors and Annette Schürmann (German Institute of Human Nutrition, Potsdam-Rehbruecke) for providing antibodies.

Appendix A. Supplementary material

Supplementary material to this article can be found online at https://doi.org/10.1016/j.jmb.2025.169189.

Received 24 February 2025;
Accepted 1 May 2025;
Available online 6 May 2025

Keywords:
ChREBP;
glucose sensing;
post-translational modification;
acetylation;
protein interactome

† Contributed equally.

Abbreviations:
ChREBP, carbohydrate response element-binding protein; LID, low-glucose inhibitory domain; NuRD, nucleosome remodeling deacetylase complex; PTMs, post-translational modifications; GRACE, glucose-response activation conserved element; GSM, glucose-sensing module; LC-MS/MS, chromatography-tandem mass spectrometry; MCRs, Mondo Conserved Regions;

NLS, nuclear localization signal; wt, Wild-type; ChoRE, carbohydrate response element; ChIP, chromatin immunoprecipitation; FDR, false discovery rate; CC, cellular components; BP, biological processes; MF, molecular function; YWHAG, 14-3-3 isoform γ; YWHAH, 14-3-3 isoform η; YWHAQ, 14-3-3 isoform θ; GO, gene ontology; ARM, tandem armadillo; NRB, LxxLL nuclear receptor box; bHLH/ZIP, basic helix-loop-helix-leucine zipper

References

[1]. Yamashita, H., Takenoshita, M., Sakurai, M., Bruick, R.K., Henzel, W.J., Shillinglaw, W., Arnot, D., Uyeda, K., (2001). A glucose-responsive transcription factor that regulates carbohydrate metabolism in the liver. *PNAS* **98**, 9116–9121.

[2]. de Luis, O., Valero, M.C., Jurado, L.A., (2000). WBSCR14, a putative transcription factor gene deleted in Williams-Beuren syndrome: complete characterisation of the human gene and the mouse ortholog. *Eur. J. Hum. Genet.* **8**, 215–222.

[3]. Cairo, S., Merla, G., Urbinati, F., Ballabio, A., Reymond, A., (2001). WBSCR14, a gene mapping to the Williams-Beuren syndrome deleted region, is a new member of the Mlx transcription factor network. *Hum. Mol. Genet.* **10**, 617–627.

[4]. Iizuka, K., Bruick, R.K., Liang, G., Horton, J.D., Uyeda, K., (2004). Deficiency of carbohydrate response element-binding protein (ChREBP) reduces lipogenesis as well as glycolysis. *PNAS* **101**, 7281–7286.

[5]. Ishii, S., Iizuka, K., Miller, B.C., Uyeda, K., (2004). Carbohydrate response element binding protein directly promotes lipogenic enzyme gene transcription. *PNAS* **101**, 15597–15602.

[6]. Poungvarin, N., Chang, B., Imamura, M., Chen, J., Moolsuwan, K., Sae-Lee, C., Li, W., Chan, L., (2015). Genome-wide analysis of ChREBP binding sites on male mouse liver and white adipose chromatin. *Endocrinology* **156**, 1982–1994.

[7]. Jeong, Y.S., Kim, D., Lee, Y.S., Kim, H.J., Han, J.Y., Im, S.S., Chong, H.K., Kwon, J.K., Cho, Y.H., Kim, W.K., Osborne, T.F., Horton, J.D., Jun, H.S., Ahn, Y.H., Ahn, S. M., Cha, J.Y., (2011). Integrated expression profiling and genome-wide analysis of ChREBP targets reveals the dual role for ChREBP in glucose-regulated gene expression. *PLoS One* **6**, e22544.

[8]. van den Berg, L., Kokki, K., Wowro, S.J., Petricek, K.M., Deniz, O., Stegmann, C.A., Robciuc, M., Teesalu, M., Melvin, R.G., Nieminen, A.I., Schupp, M., Hietakangas, V., (2023). Sugar-responsive inhibition of Myc-dependent ribosome biogenesis by Clockwork orange. *Cell Rep.* **42**, 112739.

[9]. Agius, L., (2015). Dietary carbohydrate and control of hepatic gene expression: mechanistic links from ATP and phosphate ester homeostasis to the carbohydrate-response element-binding protein. *Proc. Nutr. Soc.*, 1–9.

[10]. Abdul-Wahed, A., Guilmeau, S., Postic, C., (2017). Sweet sixteenth for ChREBP: established roles and future goals. *Cell Metab.* **26**, 324–341.

[11]. Hehl, L., Creasy, K.T., Vitali, C., Scorletti, E., Seeling, K. S., Vell, M.S., Rendel, M.D., Conlon, D., Vujkovic, M., Zandvakili, I., Trautwein, C., Schneider, K.M., Rader, D. J., Schneider, C.V., Regeneron Genetics, C., (2024). A genome-first approach to variants in MLXIPL and their association with hepatic steatosis and plasma lipids. *Hepatol. Commun.* **8**

[12]. Kooner, J.S., Chambers, J.C., Aguilar-Salinas, C.A., Hinds, D.A., Hyde, C.L., Warnes, G.R., Gomez Perez, F.J., Frazer, K.A., Elliott, P., Scott, J., Milos, P.M., Cox, D. R., Thompson, J.F., (2008). Genome-wide scan identifies variation in MLXIPL associated with plasma triglycerides. *Nature Genet.* **40**, 149–151.

[13]. Chambers, J.C., Zhang, W., Sehmi, J., Li, X., Wass, M.N., Van der Harst, P., Holm, H., Sanna, S., Kavousi, M., Baumeister, S.E., Coin, L.J., Deng, G., Gieger, C., Heard-Costa, N.L., Hottenga, J.J., Kuhnel, B., Kumar, V., Lagou, V., Liang, L., Luan, J., Vidal, P.M., Mateo Leach, I., O'Reilly, P.F., Peden, J.F., Rahmioglu, N., Soininen, P., Speliotes, E.K., Yuan, X., Thorleifsson, G., Alizadeh, B.Z., Atwood, L.D., Borecki, I.B., Brown, M.J., Charoen, P., Cucca, F., Das, D., de Geus, E.J., Dixon, A.L., Doring, A., Ehret, G., Eyjolfsson, G.I., Farrall, M., Forouhi, N.G., Friedrich, N., Goessling, W., Gudbjartsson, D.F., Harris, T.B., Hartikainen, A.L., Heath, S., Hirschfield, G.M., Hofman, A., Homuth, G., Hypponen, E., Janssen, H.L., Johnson, T., Kangas, A.J., Kema, I.P., Kuhn, J.P., Lai, S., Lathrop, M., Lerch, M.M., Li, Y., Liang, T.J., Lin, J.P., Loos, R.J., Martin, N.G., Moffatt, M.F., Montgomery, G. W., Munroe, P.B., Musunuru, K., Nakamura, Y., O'Donnell, C.J., Olafsson, I., Penninx, B.W., Pouta, A., Prins, B.P., Prokopenko, I., Puls, R., Ruokonen, A., Savolainen, M.J., Schlessinger, D., Schouten, J.N., Seedorf, U., Sen-Chowdhry, S., Siminovitch, K.A., Smit, J.H., Spector, T.D., Tan, W., Teslovich, T.M., Tukiainen, T., Uitterlinden, A.G., Van der Klauw, M.M., Vasan, R.S., Wallace, C., Wallaschofski, H., Wichmann, H.E., Willemsen, G., Wurtz, P., Xu, C., Yerges-Armstrong, L. M., Alcohol Genome-wide Association, C., Diabetes Genetics, R., Meta-analyses, S., Genetic Investigation of Anthropometric Traits, C., Global Lipids Genetics, C., Genetics of Liver Disease, C., International Consortium for Blood, P., Meta-analyses of, G., Insulin-Related Traits, C., Abecasis, G.R., Ahmadi, K.R., Boomsma, D.I., Caulfield, M., Cookson, W.O., van Duijn, C.M., Froguel, P., Matsuda, K., McCarthy, M.I., Meisinger, C., Mooser, V., Pietilainen, K.H., Schumann, G., Snieder, H., Sternberg, M.J., Stolk, R.P., Thomas, H.C., Thorsteinsdottir, U., Uda, M., Waeber, G., Wareham, N. J., Waterworth, D.M., Watkins, H., Whitfield, J.B., Witteman, J.C., Wolffenbuttel, B.H., Fox, C.S., Ala-Korpela, M., Stefansson, K., Vollenweider, P., Volzke, H., Schadt, E.E., Scott, J., Jarvelin, M.R., Elliott, P., Kooner, J.S., (2011). Genome-wide association study identifies loci influencing concentrations of liver enzymes in plasma. *Nature Genet.* **43**, 1131–1138.

[14]. Eissing, L., Scherer, T., Todter, K., Knippschild, U., Greve, J.W., Buurman, W.A., Pinnschmidt, H.O., Rensen, S.S., Wolf, A.M., Bartelt, A., Heeren, J., Buettner, C., Scheja, L., (2013). De novo lipogenesis in human fat and liver is linked to ChREBP-beta and metabolic health. *Nature Commun.* **4**, 1528.

[15]. Kursawe, R., Caprio, S., Giannini, C., Narayan, D., Lin, A., D'Adamo, E., Shaw, M., Pierpont, B., Cushman, S.W., Shulman, G.I., (2013). Decreased transcription of ChREBP-alpha/beta isoforms in abdominal subcutaneous adipose tissue of obese adolescents with

prediabetes or early type 2 diabetes: associations with insulin resistance and hyperglycemia. *Diabetes* **62**, 837–844.

[16]. Willems, S.M., Ng, N.H.J., Fernandez, J., Fine, R.S., Wheeler, E., Wessel, J., Kitajima, H., Marenne, G., Sim, X., Yaghootkar, H., Wang, S., Chen, S., Chen, Y., Chen, Y.I., Grarup, N., Li-Gao, R., Varga, T.V., Asimit, J.L., Feng, S., Strawbridge, R.J., Kleinbrink, E.L., Ahluwalia, T. S., An, P., Appel, E.V., Arking, D.E., Auvinen, J., Bielak, L.F., Bihlmeyer, N.A., Bork-Jensen, J., Brody, J.A., Campbell, A., Chu, A.Y., Davies, G., Demirkan, A., Floyd, J.S., Giulianini, F., Guo, X., Gustafsson, S., Jackson, A.U., Jakobsdottir, J., Jarvelin, M.R., Jensen, R.A., Kanoni, S., Keinanen-Kiukaanniemi, S., Li, M., Lu, Y., Luan, J., Manning, A.K., Marten, J., Meidtner, K., Mook-Kanamori, D.O., Muka, T., Pistis, G., Prins, B., Rice, K.M., Sanna, S., Smith, A.V., Smith, J.A., Southam, L., Stringham, H.M., Tragante, V., van der Laan, S.W., Warren, H.R., Yao, J., Yiorkas, A.M., Zhang, W., Zhao, W., Graff, M., Highland, H.M., Justice, A.E., Marouli, E., Medina-Gomez, C., Afaq, S., Alhejily, W.A., Amin, N., Asselbergs, F.W., Bonnycastle, L.L., Bots, M.L., Brandslund, I., Chen, J., Danesh, J., de Mutsert, R., Dehghan, A., Ebeling, T., Elliott, P., Consortium, E.P.-I., Farmaki, A.E., Faul, J.D., Franks, P.W., Franks, S., Fritsche, A., Gjesing, A.P., Goodarzi, M.O., Gudnason, V., Hallmans, G., Harris, T.B., Herzig, K.H., Hivert, M.F., Jorgensen, T., Jorgensen, M.E., Jousilahti, P., Kajantie, E., Karaleftheri, M., Kardia, S.L.R., Kinnunen, L., Koistinen, H.A., Komulainen, P., Kovacs, P., Kuusisto, J., Laakso, M., Lange, L.A., Launer, L.J., Leong, A., Lindstrom, J., Manning Fox, J.E., Mannisto, S., Maruthur, N.M., Moilanen, L., Mulas, A., Nalls, M.A., Neville, M., Pankow, J.S., Pattie, A., Petersen, E.R.B., Puolijoki, H., Rasheed, A., Redmond, P., Renstrom, F., Roden, M., Saleheen, D., Saltevo, J., Savonen, K., Sebert, S., Skaaby, T., Small, K.S., Stancakova, A., Stokholm, J., Strauch, K., Tai, E.S., Taylor, K.D., Thuesen, B.H., Tonjes, A., Tsafantakis, E., Tuomi, T., Tuomilehto, J., Understanding Society Scientific, G., Uusitupa, M., Vaarasmaki, M., Vaartjes, I., Zoledziewska, M., Abecasis, G., Balkau, B., Bisgaard, H., Blakemore, A.I., Bluher, M., Boeing, H., Boerwinkle, E., Bonnelykke, K., Bottinger, E.P., Caulfield, M.J., Chambers, J.C., Chasman, D.I., Cheng, C.Y., Collins, F.S., Coresh, J., Cucca, F., de Borst, G.J., Deary, I.J., Dedoussis, G., Deloukas, P., den Ruijter, H.M., Dupuis, J., Evans, M.K., Ferrannini, E., Franco, O.H., Grallert, H., Hansen, T., Hattersley, A.T., Hayward, C., Hirschhorn, J.N., Ikram, A., Ingelsson, E., Karpe, F., Kaw, K.T., Kiess, W., Kooner, J. S., Korner, A., Lakka, T., Langenberg, C., Lind, L., Lindgren, C.M., Linneberg, A., Lipovich, L., Liu, C.T., Liu, J., Liu, Y., Loos, R.J.F., MacDonald, P.E., Mohlke, K. L., Morris, A.D., Munroe, P.B., Murray, A., Padmanabhan, S., Palmer, C.N.A., Pasterkamp, G., Pedersen, O., Peyser, P.A., Polasek, O., Porteous, D., Province, M.A., Psaty, B.M., Rauramaa, R., Ridker, P.M., Rolandsson, O., Rorsman, P., Rosendaal, F.R., Rudan, I., Salomaa, V., Schulze, M.B., Sladek, R., Smith, B.H., Spector, T.D., Starr, J.M., Stumvoll, M., van Duijn, C.M., Walker, M., Wareham, N.J., Weir, D.R., Wilson, J.G., Wong, T.Y., Zeggini, E., Zonderman, A.B., Rotter, J.I., Morris, A.P., Boehnke, M., Florez, J.C., McCarthy, M.I., Meigs, J.B., Mahajan, A., Scott, R.A., Gloyn, A.L., Barroso, I., (2023). Large-scale exome array summary statistics resources for glycemic traits to aid effector gene prioritization. *Wellcome Open Res.* **8**, 483.

[17]. Gardner, E.J., Kentistou, K.A., Stankovic, S., Lockhart, S., Wheeler, E., Day, F.R., Kerrison, N.D., Wareham, N. J., Langenberg, C., O'Rahilly, S., Ong, K.K., Perry, J.R.B., (2022). Damaging missense variants in IGF1R implicate a role for IGF-1 resistance in the etiology of type 2 diabetes. *Cell Genom.* **2**

[18]. Katz, L.S., Baumel-Alterzon, S., Scott, D.K., Herman, M. A., (2021). Adaptive and maladaptive roles for ChREBP in the liver and pancreatic islets. *J. Biol. Chem.* **296**, 100623.

[19]. Regnier, M., Carbinatti, T., Parlati, L., Benhamed, F., Postic, C., (2023). The role of ChREBP in carbohydrate sensing and NAFLD development. *Nature Rev. Endocrinol.* **19**, 336–349.

[20]. Ge, Q., Huang, N., Wynn, R.M., Li, Y., Du, X., Miller, B., Zhang, H., Uyeda, K., (2012). Structural characterization of a unique interface between carbohydrate response element-binding protein (ChREBP) and 14-3-3beta protein. *J. Biol. Chem.* **287**, 41914–41921.

[21]. Nakagawa, T., Ge, Q., Pawlosky, R., Wynn, R.M., Veech, R.L., Uyeda, K., (2013). Metabolite regulation of nucleo-cytosolic trafficking of carbohydrate response element-binding protein (ChREBP): role of ketone bodies. *J. Biol. Chem.* **288**, 28358–28367.

[22]. Sato, S., Jung, H., Nakagawa, T., Pawlosky, R., Takeshima, T., Lee, W.R., Sakiyama, H., Laxman, S., Wynn, R.M., Tu, B.P., MacMillan, J.B., De Brabander, J. K., Veech, R.L., Uyeda, K., (2016). Metabolite regulation of nuclear localization of carbohydrate-response element-binding protein (ChREBP): role of AMP as an allosteric inhibitor. *J. Biol. Chem.* **291**, 10515–10527.

[23]. Jung, H., Takeshima, T., Nakagawa, T., MacMillan, K., Wynn, R.M., Wang, H., Sakiyama, H., Wei, S., Li, Y., Bruick, R.K., Posner, B.A., De Brabander, J.K., Uyeda, K., (2020). The Structure of Importin alpha and the nuclear localization peptide of ChREBP, and small compound inhibitors of ChREBP-Importin alpha interactions. *Biochem. J.*.

[24]. Davies, M.N., O'Callaghan, B.L., Towle, H.C., (2008). Glucose activates ChREBP by increasing its rate of nuclear entry and relieving repression of its transcriptional activity. *J. Biol. Chem.* **283**, 24029–24038.

[25]. Heidenreich, S., Weber, P., Stephanowitz, H., Petricek, K. M., Schutte, T., Oster, M., Salo, A.M., Knauer, M., Goehring, I., Yang, N., Witte, N., Schumann, A., Sommerfeld, M., Muenzner, M., Myllyharju, J., Krause, E., Schupp, M., (2020). The glucose-sensing transcription factor ChREBP is targeted by proline hydroxylation. *J. Biol. Chem.* **295**, 17158–17168.

[26]. Li, M.V., Chang, B., Imamura, M., Poungvarin, N., Chan, L., (2006). Glucose-dependent transcriptional regulation by an evolutionarily conserved glucose-sensing module. *Diabetes* **55**, 1179–1189.

[27]. McFerrin, L.G., Atchley, W.R., (2012). A novel N-terminal domain may dictate the glucose response of Mondo proteins. *PLoS One* **7**, e34803.

[28]. Bricambert, J., Miranda, J., Benhamed, F., Girard, J., Postic, C., Dentin, R., (2010). Salt-inducible kinase 2 links transcriptional coactivator p300 phosphorylation to the prevention of ChREBP-dependent hepatic steatosis in mice. *J. Clin. Invest.* **120**, 4316–4331.

[29]. Cha-Molstad, H., Saxena, G., Chen, J., Shalev, A., (2009). Glucose-stimulated expression of Txnip is mediated by carbohydrate response element-binding protein, p300, and histone H4 acetylation in pancreatic beta cells. *J. Biol. Chem.* **284**, 16898–16905.

[30]. Marmier, S., Dentin, R., Daujat-Chavanieu, M., Guillou, H., Bertrand-Michel, J., Gerbal-Chaloin, S., Girard, J., Lotersztajn, S., Postic, C., (2015). Novel role for carbohydrate responsive element binding protein in the control of ethanol metabolism and susceptibility to binge drinking. *Hepatology* **62**, 1086–1100.

[31]. Schneider, C.A., Rasband, W.S., Eliceiri, K.W., (2012). NIH Image to ImageJ: 25 years of image analysis. *Nature Methods* **9**, 671–675.

[32]. Tsatsos, N.G., Towle, H.C., (2006). Glucose activation of ChREBP in hepatocytes occurs via a two-step mechanism. *Biochem. Biophys. Res. Commun.* **340**, 449–456.

[33]. Oster, M., Galhuber, M., Krstic, J., Steinhoff, J.S., Lenihan-Geels, G., Wulff, S., Kiefer, M.F., Petricek, K. M., Wowro, S.J., Flores, R.E., Yang, N., Li, C., Meng, Y., Reinisch, I., Sommerfeld, M., Weger, S., Habisch, H., Madl, T., Schulz, T.J., Prokesch, A., Schupp, M., (2022). Hepatic p53 is regulated by transcription factor FOXO1 and acutely controls glycogen homeostasis. *J. Biol. Chem.* **298**, 102287.

[34]. Su, A.I., Wiltshire, T., Batalov, S., Lapp, H., Ching, K.A., Block, D., Zhang, J., Soden, R., Hayakawa, M., Kreiman, G., Cooke, M.P., Walker, J.R., Hogenesch, J.B., (2004). A gene atlas of the mouse and human protein-encoding transcriptomes. *PNAS* **101**, 6062–6067.

[35]. Uhlen, M., Fagerberg, L., Hallstrom, B.M., Lindskog, C., Oksvold, P., Mardinoglu, A., Sivertsson, A., Kampf, C., Sjostedt, E., Asplund, A., Olsson, I., Edlund, K., Lundberg, E., Navani, S., Szigyarto, C.A., Odeberg, J., Djureinovic, D., Takanen, J.O., Hober, S., Alm, T., Edqvist, P.H., Berling, H., Tegel, H., Mulder, J., Rockberg, J., Nilsson, P., Schwenk, J.M., Hamsten, M., von Feilitzen, K., Forsberg, M., Persson, L., Johansson, F., Zwahlen, M., von Heijne, G., Nielsen, J., Ponten, F., (2015). Proteomics. Tissue-based map of the human proteome. *Science* **347**, 1260419.

[36]. Del Toro, N., Shrivastava, A., Ragueneau, E., Meldal, B., Combe, C., Barrera, E., Perfetto, L., How, K., Ratan, P., Shirodkar, G., Lu, O., Meszaros, B., Watkins, X., Pundir, S., Licata, L., Iannuccelli, M., Pellegrini, M., Martin, M.J., Panni, S., Duesbury, M., Vallet, S.D., Rappsilber, J., Ricard-Blum, S., Cesareni, G., Salwinski, L., Orchard, S., Porras, P., Panneerselvam, K., Hermjakob, H., (2022). The IntAct database: efficient access to fine-grained molecular interaction data. *Nucleic Acids Res.* **50**, D648–D653.

[37]. Hulsen, T., de Vlieg, J., Alkema, W., (2008). BioVenn – a web application for the comparison and visualization of biological lists using area-proportional Venn diagrams. *BMC Genomics* **9**, 488.

[38]. Chen, E.Y., Tan, C.M., Kou, Y., Duan, Q., Wang, Z., Meirelles, G.V., Clark, N.R., Ma'ayan, A., (2013). Enrichr: interactive and collaborative HTML5 gene list enrichment analysis tool. *BMC Bioinf.* **14**, 128.

[39]. Xue, X., Zhang, W., Fan, A., (2023). Comparative analysis of gene ontology-based semantic similarity measurements for the application of identifying essential proteins. *PLoS One* **18**, e0284274.

[40]. Eilers, A.L., Sundwall, E., Lin, M., Sullivan, A.A., Ayer, D. E., (2002). A novel heterodimerization domain, CRM1, and 14-3-3 control subcellular localization of the MondoA-Mlx heterocomplex. *Mol. Cell Biol.* **22**, 8514–8526.

[41]. Li, M.V., Chen, W., Poungvarin, N., Imamura, M., Chan, L., (2008). Glucose-mediated transactivation of carbohydrate response element-binding protein requires cooperative actions from Mondo conserved regions and essential trans-acting factor 14-3-3. *Mol. Endocrinol.* **22**, 1658–1672.

[42]. Herman, M.A., Peroni, O.D., Villoria, J., Schon, M.R., Abumrad, N.A., Bluher, M., Klein, S., Kahn, B.B., (2012). A novel ChREBP isoform in adipose tissue regulates systemic glucose metabolism. *Nature* **484**, 333–338.

[43]. Ge, Q., Nakagawa, T., Wynn, R.M., Chook, Y.M., Miller, B.C., Uyeda, K., (2011). Importin-alpha protein binding to a nuclear localization signal of carbohydrate response element-binding protein (ChREBP). *J. Biol. Chem.* **286**, 28119–28127.

[44]. Pang, S.T., Hsieh, W.C., Chuang, C.K., Chao, C.H., Weng, W.H., Juang, H.H., (2009). Thioredoxin-interacting protein: an oxidative stress-related gene is upregulated by glucose in human prostate carcinoma cells. *J. Mol. Endocrinol.* **42**, 205–214.

[45]. Pashkov, V., Huang, J., Parameswara, V.K., Kedzierski, W., Kurrasch, D.M., Tall, G.G., Esser, V., Gerard, R.D., Uyeda, K., Towle, H.C., Wilkie, T.M., (2011). Regulator of G protein signaling (RGS16) inhibits hepatic fatty acid oxidation in a carbohydrate response element-binding protein (ChREBP)-dependent manner. *J. Biol. Chem.* **286**, 15116–15125.

[46]. Wu, J.C., Merlino, G., Fausto, N., (1994). Establishment and characterization of differentiated, nontransformed hepatocyte cell lines derived from mice transgenic for transforming growth factor alpha. *PNAS* **91**, 674–678.

[47]. Nishimura, D., (2001). BioCarta. *Biotech. Softw. Internet Rep.* **2**, 117–120.

[48]. Sakin, V., Richter, S.M., Hsiao, H.H., Urlaub, H., Melchior, F., (2015). Sumoylation of the GTPase ran by the RanBP2 SUMO E3 ligase complex. *J. Biol. Chem.* **290**, 23589–23602.

[49]. Paysan-Lafosse, T., Blum, M., Chuguransky, S., Grego, T., Pinto, B.L., Salazar, G.A., Bileschi, M.L., Bork, P., Bridge, A., Colwell, L., Gough, J., Haft, D.H., Letunic, I., Marchler-Bauer, A., Mi, H., Natale, D.A., Orengo, C.A., Pandurangan, A.P., Rivoire, C., Sigrist, C.J.A., Sillitoe, I., Thanki, N., Thomas, P.D., Tosatto, S.C.E., Wu, C.H., Bateman, A., (2023). InterPro in 2022. *Nucleic Acids Res.* **51**, D418–D427.

[50]. Ichimura, T., Isobe, T., Okuyama, T., Takahashi, N., Araki, K., Kuwano, R., Takahashi, Y., (1988). Molecular cloning of cDNA coding for brain-specific 14-3-3 protein, a protein kinase-dependent activator of tyrosine and tryptophan hydroxylases. *PNAS* **85**, 7084–7088.

[51]. Han, H., Cho, J.W., Lee, S., Yun, A., Kim, H., Bae, D., Yang, S., Kim, C.Y., Lee, M., Kim, E., Lee, S., Kang, B., Jeong, D., Kim, Y., Jeon, H.N., Jung, H., Nam, S., Chung, M., Kim, J.H., Lee, I., (2018). TRRUST v2: an expanded reference database of human and mouse transcriptional regulatory interactions. *Nucleic Acids Res.* **46**, D380–D386.

[52]. Wang, H., Stevens, T., Lu, J., Roberts, A., Van't Land, C., Muzumdar, R., Gong, Z., Vockley, J., Prochownik, E.V., (2024). Body-wide inactivation of the Myc-Like Mlx

transcription factor network accelerates aging and increases the lifetime cancer incidence. *Adv. Sci. (Weinh.)*e2401593.

[53]. Zhang, P., Metukuri, M.R., Bindom, S.M., Prochownik, E. V., O'Doherty, R.M., Scott, D.K., (2010). c-Myc is required for the CHREBP-dependent activation of glucose-responsive genes. *Mol. Endocrinol.* **24**, 1274–1286.

[54]. Wang, H., Dolezal, J.M., Kulkarni, S., Lu, J., Mandel, J., Jackson, L.E., Alencastro, F., Duncan, A.W., Prochownik, E.V., (2018). Myc and ChREBP transcription factors cooperatively regulate normal and neoplastic hepatocyte proliferation in mice. *J. Biol. Chem.* **293**, 14740–14757.

[55]. Sayols, S., (2023). rrvgo: a bioconductor package for interpreting lists of gene ontology terms. *MicroPubl. Biol.* **2023**

[56]. Merla, G., Howald, C., Antonarakis, S.E., Reymond, A., (2004). The subcellular localization of the ChoRE-binding protein, encoded by the Williams-Beuren syndrome critical region gene 14, is regulated by 14-3-3. *Hum. Mol. Genet.* **13**, 1505–1514.

[57]. Sakiyama, H., Wynn, R.M., Lee, W.R., Fukasawa, M., Mizuguchi, H., Gardner, K.H., Repa, J.J., Uyeda, K., (2008). Regulation of nuclear import/export of carbohydrate response element-binding protein (ChREBP): interaction of an alpha-helix of ChREBP with the 14-3-3 proteins and regulation by phosphorylation. *J. Biol. Chem.* **283**, 24899–24908.

[58]. Moroianu, J., Blobel, G., (1995). Protein export from the nucleus requires the GTPase Ran and GTP hydrolysis. *PNAS* **92**, 4318–4322.

[59]. Wagner, T., Brand, P., Heinzel, T., Kramer, O.H., (2014). Histone deacetylase 2 controls p53 and is a critical factor in tumorigenesis. *BBA* **1846**, 524–538.

[60]. Chen, Y., Wu, R., Chen, H.Z., Xiao, Q., Wang, W.J., He, J.P., Li, X.X., Yu, X.W., Li, L., Wang, P., Wan, X.C., Tian, X.H., Li, S.J., Yu, X., Wu, Q., (2015). Enhancement of hypothalamic STAT3 acetylation by nuclear receptor Nur77 dictates leptin sensitivity. *Diabetes* **64**, 2069–2081.

[61]. Trivedi, C.M., Zhu, W., Wang, Q., Jia, C., Kee, H.J., Li, L., Hannenhalli, S., Epstein, J.A., (2010). Hopx and Hdac2 interact to modulate Gata4 acetylation and embryonic cardiac myocyte proliferation. *Dev. Cell* **19**, 450–459.

[62]. Bornelov, S., Reynolds, N., Xenophontos, M., Gharbi, S., Johnstone, E., Floyd, R., Ralser, M., Signolet, J., Loos, R., Dietmann, S., Bertone, P., Hendrich, B., (2018). The nucleosome remodeling and deacetylation complex modulates chromatin structure at sites of active transcription to fine-tune gene expression. *Mol. Cell* **71**, 56–72.e54.

[63]. Witte, N., Muenzner, M., Rietscher, J., Knauer, M., Heidenreich, S., Nuotio-Antar, A.M., Graef, F.A., Fedders, R., Tolkachov, A., Goehring, I., Schupp, M., (2015). The glucose sensor ChREBP links de Novo lipogenesis to PPARgamma activity and adipocyte differentiation. *Endocrinology* **156**, 4008–4019.

[64]. Nuotio-Antar, A.M., Poungvarin, N., Li, M., Schupp, M., Mohammad, M., Gerard, S., Zou, F., Chan, L., (2015). FABP4-Cre mediated expression of constitutively active ChREBP protects against obesity, fatty liver, and insulin resistance. *Endocrinology* **156**, 4020–4032.

[65]. Rikova, K., Guo, A., Zeng, Q., Possemato, A., Yu, J., Haack, H., Nardone, J., Lee, K., Reeves, C., Li, Y., Hu, Y., Tan, Z., Stokes, M., Sullivan, L., Mitchell, J., Wetzel, R., Macneill, J., Ren, J.M., Yuan, J., Bakalarski, C.E., Villen, J., Kornhauser, J.M., Smith, B., Li, D., Zhou, X., Gygi, S. P., Gu, T.L., Polakiewicz, R.D., Rush, J., Comb, M.J., (2007). Global survey of phosphotyrosine signaling identifies oncogenic kinases in lung cancer. *Cell* **131**, 1190–1203.

[66]. Hornbeck, P.V., Zhang, B., Murray, B., Kornhauser, J.M., Latham, V., Skrzypek, E., (2015). PhosphoSitePlus, 2014: mutations, PTMs and recalibrations. *Nucleic Acids Res.* **43**, D512–D520.